

# Solvent-Free Synthesis, Characterization, and Antimicrobial Activity of Transition Metal Complexes of Schiff Base Ligand Derived from 6-iodo-4-oxo-4H-chromene-3-carbaldehyde with 4-Methyl-1,2,3-thiadiazole-5-carbohydrazide

Ram B. Kohire <sup>1</sup>, Dnyaneshwar T. Nagre <sup>2</sup>, Amol D. Kale <sup>3</sup>, Sushil K. Ghumbre <sup>4</sup>,  
Sadashiv N. Sinkar <sup>5,\*</sup>

<sup>1</sup> Department of Chemistry Swami Vivakanand Sr. College Mantha, Dist. Jalna (M.S.), India; kohireram@rediffmail.com;

<sup>2</sup> Department of Chemistry RMIG College, Jalna (M.S.), India; nelsy.nagre@gmail.com;

<sup>3</sup> Department of Chemistry Swami Vivakanand Sr. College Mantha, Dist. Jalna (M.S.), India; indiakaleamo009@gmail.com;

<sup>4</sup> Department of Chemistry I.C.S. College of Art's, Commerce and Science, Khed. India; sghumbre6680@gmail.com;

<sup>5</sup> \*Department of Chemistry MSS'S Arts Science and Commerce College Ambad, Dist. Jalna. (M.S.), India; sadachem@rediffmail.com;

\* Correspondence: sadachem@rediffmail.com;

Scopus Author ID 6506207573

Received: 8.06.2024; Accepted: 6.10.2024; Published: 14.02.2025

**Abstract:** A Schiff base ligand derived from 6-iodo-4-oxo-4H-chromen-3-yl)methylene)-4-methyl-1,2,3-thiadiazole-5-carbohydrazide was synthesized, along with its transition metal complexes of Ru(III), Rh(II), Pd(II), Ag(II), and Cd(II), using microwave irradiation as a green approach, contrasting with conventional methods. The structures of these compounds were thoroughly characterized through elemental and spectroscopic analyses, including IR, <sup>1</sup>H-NMR, XRD, and electronic spectra, elucidating their geometrical arrangements. Furthermore, the thermal stability of the Pd(II), Ag(II), and Cd(II) complexes was investigated via thermo-gravimetric analyses (TGA). Elemental analysis confirmed a metal-to-ligand stoichiometry of 1:2 molar ratio. Additionally, the complexes were screened for their potential biological activities, particularly antimicrobial properties.

**Keywords:** microwave synthesis; Schiff base ligand; thermal study; biological activity.

© 2024 by the authors. This article is an open-access article distributed under the terms and conditions of the Creative Commons Attribution (CC BY) license (<https://creativecommons.org/licenses/by/4.0/>).

## 1. Introduction

Chromone hydrazones are extremely promising ligands in coordination chemistry, and the biological properties of their metal complexes have been growing in recent years [1-2]. The coordination chemistry of transition metals with ligands from the hydrazone family has been of interest due to the different bonding modes shown by these ligands [3]. Generally, the possible donor sites in hydrazones are amide oxygen and azomethine nitrogen [4]. However, the possibility remains of generating complexes with new molecular architectures by suitable substitution in the carbonyl and hydrazide part [5]. This is partially due to their capability of acting as NO, ONO, NNO, and ONNO donors with the formation of either mono/bi or polynuclear complexes [6-8]. Chromone hydrazones and their derivative analogs that have potential biological activity are the focus of extensive investigation [9]. Specifically, the chromone hydrazones have been screened for their antifungal, antibacterial, antioxidant,

antimalarial, anti-inflammatory, and DNA binding [10]. Considering the above points and considering the biological potentials of hydrazones [11]. We have synthesized eight chromone hydrazones. The two chromones (3-formyl chromone and 6-methyl-3-formyl chromones) selected here have a keto group, which provides a further binding site for metal cations and behaves as chelating ligands. The spectroscopic data showed that the ONO/NO donor ligands act as monobasic tri/bidentate chelates [12-13]. The coordination sites with the metal (II) ion are pyrone oxygen, azomethine nitrogen, and hydrazonic oxygen [14]. The ligand systems of our interest and their abbreviations are as follows. Microwave-assisted synthesis is considered one of the most crucial subdivisions of green chemistry [15]. Microwave reactions under free or less solvent conditions are eye-catching and present reduced pollution, low price, and high productivity, with easy processing and handling [16-17].

## 2. Materials and Methods

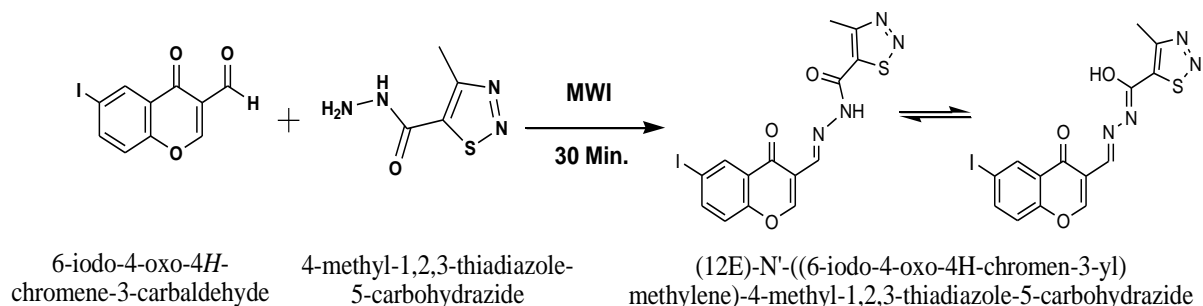
All the analytical grades, reagents, and chemicals were used without further purification. Solvents were purified and dried according to the literature method [18]. All chemicals were obtained from Sigma-Aldrich and used without purification. The 6-iodo-4-oxo-4H-chromene-3-carbaldehyde and 4-Methyl-1,2,3,-thiadiazole-5-carbohydrazide; the remaining all chemical solvents were purchased from Spectrochem Ltd.

### 2.1. Physical measurements.

Elemental analysis (C, H, N) was performed using the Perkin Elmer CHN analyzer. IR spectra of the ligands and their metal complexes were recorded on Bruker spectrometer within the range of 4000-400  $\text{cm}^{-1}$ . Thermal studies of the complexes were carried out using a Perkin Elmer diamond TGA instrument.  $^1\text{H-NMR}$  spectra of the ligands were recorded on Bruker spectrometer using DMSO- $d_6$  as a solvent and TMS as an internal standard. Mass spectra were recorded on water, Qt of micromass (ESI-MS).

### 2.2. Synthesis of Schiff base ligand.

The Schiff base ligand has been synthesized by reacting 6-iodo-4-oxo-4H-chromene-3-carbaldehyde (1.00 mmole) and 4-Methyl-1,2,3,-thiadiazole-5-carbohydrazide (1.00 mmole). The reaction was carried out in a microwave oven for 30 minutes. The irradiated product was washed with dry ether and filtered. The final product was recrystallized from ethanol to give pale yellow crystals. The product's purity was monitored by using TLC, n-hexane, and ethyl acetate (7:3) (Scheme 1)[19].



Scheme 1: The schematic route for the synthesis of Schiff base Ligand (L).



oxygen atom of the carbonyl group of the chromone moiety[22]. The stretching vibration of the azomethine group (C=N) was observed at 1574 cm<sup>-1</sup> in the ligand. This band was shifted to the lower wavenumber region 25-40 cm<sup>-1</sup> in their metal complexes, indicating the participation of the nitrogen atom of the azomethine group in coordination with the metal ion. The appearance of new broadband in the region 3234-3409 cm<sup>-1</sup> indicates the presence of coordinated water in Ag(II) and Cd(II) metal complexes. The coordination of nitrogen and oxygen atoms was supported by the appearance of non-ligand bands in the range 520-538 cm<sup>-1</sup> and 422-462 cm<sup>-1</sup> region due to the  $\nu(\text{M-O})$  and  $\nu(\text{M-N})$ , respectively. From the above spectral data, it was concluded that Schiff base ligand acts as bidentate with coordinate two water molecules in Ag(II) and Cd(II) metal complexes and tridentate ligands in Ru(III), Rh(II). The FT-IR spectral data containing relevant vibrational bands of the ligands and their metal complexes are listed in Table 2.

**Table 2.** The selective infrared frequencies of ligand (L) and its metal complexes.

Compound Name	$\nu(\text{C=O})$ Chromone	$\nu(\text{C=O})$ hydrozonic	$\nu(\text{C=N})$	$\nu(\text{M-O})$	$\nu(\text{M-N})$
L	1665	1625	1574	-	
[Ru(L) <sub>2</sub> ]	1656	1603	1533	520	422
[Rh(L) <sub>2</sub> ]	1633	1616	1530	512	418
[Pd(L) <sub>2</sub> ]	1654	1605	1562	510	412
[Ag(L) <sub>2</sub> (H <sub>2</sub> O) <sub>2</sub> ]	1697	1627	1587	538	422
[Cd(L) <sub>2</sub> (H <sub>2</sub> O) <sub>2</sub> ]	1669	1632	1595	524	462

### 3.2. Electronic spectra.

The electronic spectral data of the ligand (chromone hydrazone) in DMF (10<sup>-3</sup>M) (Table.3) showed two bands with  $\lambda_{\text{max}}$  (DMF) 313-356 nm (32573-32154 cm<sup>-1</sup>) and 342-361 nm (29239-27700 cm<sup>-1</sup>) for chromone hydrazone ligands. The higher energy band may be assigned to  $\pi\text{-}\pi^*$  transitions of the azomethine linkage and the aromatic rings[23]. The medium energy band may be assigned to  $n\text{-}\pi^*$  transitions of the C=O and C=N groups. UV-Visible spectral data is represented in Table 3.

**Table 3.** UV-visible spectral data of chromone hydrazone ligands in DMF (10<sup>-3</sup>M).

No	Compounds	Electronic spectral bands (nm)
		$\lambda_{\text{max}}$ (nm)/( $\epsilon_{\text{max}} \times 10^3 \text{ L cm}^{-1} \text{ mol}^{-1}$ )
1	L	313 (1.31) - $\pi\text{-}\pi^*$
		356 (5.2) - $n\text{-}\pi^*$

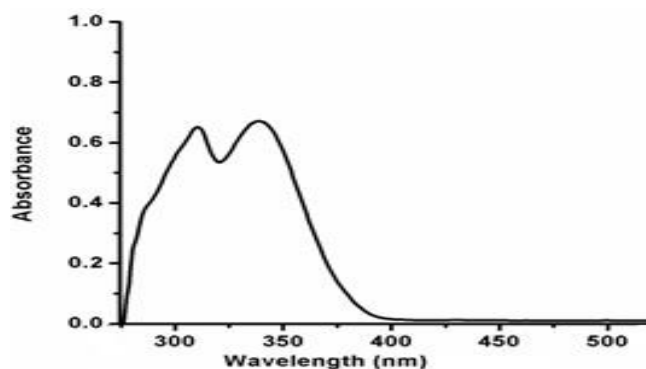


**Figure 1.** UV-visible Spectrum of Schiff base ligand (L).

### 3.3. <sup>1</sup>H-NMR spectra.

The <sup>1</sup>H-NMR spectrums of ligand and metal complexes were recorded in DMSO-d<sub>6</sub>. The spectrum of ligand shows following signals: <sup>1</sup>H- NMR (DMSO-d<sub>6</sub>, δ ppm ) 12.36 (1H,s, iminolic -OH); 8.47 (S, 1H, HC=N), 6.94-8.26 (m, 4H, Ar-H); 2.98 (S, 3H, -CH<sub>3</sub>);[24].

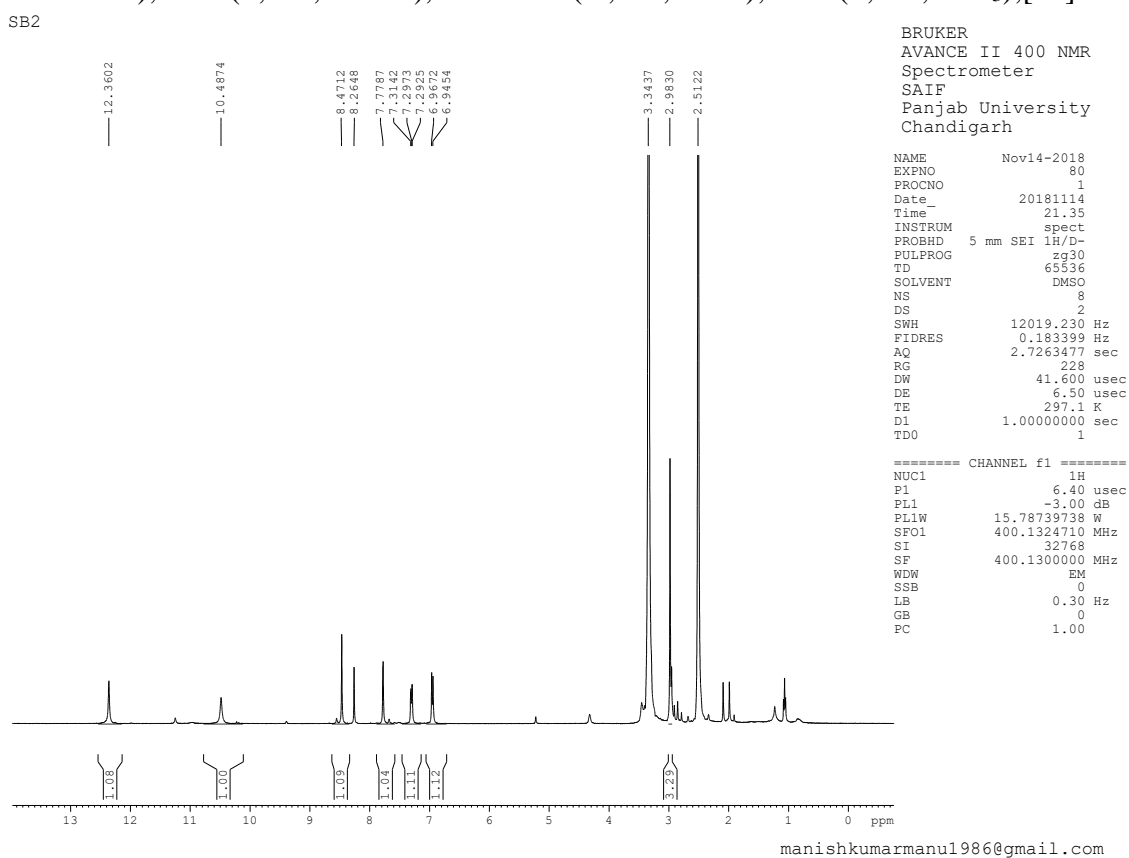


**Figure 2.** <sup>1</sup>H-NMR spectrums of Schiff base ligand.

### 3.4. Thermo gravimetric analysis.

Thermal analysis was used mainly to confirm the water molecule or solvent associated with being in the sphere of coordination or the outer sphere of the complex [25] and the information about its properties and the nature of the product's intermediate and final thermal decomposition. From the TGA curves, the weight loss was calculated for the different steps and compared with the theoretically calculated weight for the suggested formulas based on the results obtained from the elemental analyses. Thermal stability of the synthesized metal complexes was done up to 900°C at a heating rate of 10°C/min in a nitrogen atmosphere. Metal complexes exhibit similar decomposition patterns, as is evident from their TGA graphs. The TGA graph shows the decomposition of the Ru metal complex in two steps within a temperature range of 10-700°C. The first step corresponds to the loss of (C<sub>11</sub>H<sub>7</sub>IN<sub>2</sub>O<sub>3</sub>)<sub>2</sub> (Found 68.44 %, calc. 69.65 %) in the temperature range of 230-420°C. The second step corresponds to the loss of (C<sub>3</sub>H<sub>4</sub>N<sub>2</sub>S)<sub>2</sub> (Found 19.78 %, calc. 20.43 %) in the temperature range of 400-600°C. The third step, which is the final product, leaves RuO as residue. The TGA graph shows the decomposition of the Cd metal complex in three steps within a temperature range of 10-700°C. The first step corresponds to losing two coordinated water molecules (Found 3.10%, calc. 3.63 %) in the temperature range of 10-80°C. The second step corresponds to the loss of (C<sub>11</sub>H<sub>7</sub>IN<sub>2</sub>O<sub>3</sub>)<sub>2</sub> (Found 67.76 %, calc. 68.81 %) in the temperature range of 200-400°C. A peak

corresponding to mass loss of (19.68% calcd.20.18 %) at 400-580°C was due to the loss of (C<sub>3</sub>H<sub>4</sub>N<sub>2</sub>S)<sub>2</sub> in the third step, and as a final product, it leaves CdO as residue.

**Table 4.** Thermal analysis data of metal complexes.

Comp. No.	Molecular formula	Stages	Temp(°c)	Possible evolved species	Mass loss in (%)		Residue species
					Found	Calc.	
1	C <sub>28</sub> H <sub>16</sub> I <sub>2</sub> N <sub>6</sub> RuS <sub>2</sub> (979)	1 <sup>st</sup>	230-420	(C <sub>11</sub> H <sub>7</sub> IN <sub>2</sub> O <sub>3</sub> ) <sub>2</sub>	68.44	69.65	RuO
		2 <sup>nd</sup>	400-600	(C <sub>3</sub> H <sub>4</sub> N <sub>2</sub> S) <sub>2</sub>	19.78	20.43	
		3 <sup>rd</sup>	600-700		10.80	11.95	
2	C <sub>28</sub> H <sub>16</sub> CdI <sub>2</sub> N <sub>8</sub> N <sub>8</sub> O <sub>6</sub> S <sub>2</sub> (991)	1 <sup>st</sup>	10-180	2H <sub>2</sub> O	3.10	3.63	CdO
		2 <sup>nd</sup>	200-400	(C <sub>11</sub> H <sub>7</sub> IN <sub>2</sub> O <sub>3</sub> ) <sub>2</sub>	67.76	68.81	
		3 <sup>rd</sup>	400-580	(C <sub>3</sub> H <sub>4</sub> N <sub>2</sub> S) <sub>2</sub>	19.68	20.18	
		4 <sup>th</sup>	580-700		12.14	13.01	

### 3.5. Powder XRD studies.

The X-ray diffractograms of Ru(II) and Cd(II) complexes were recorded between 5-80° at wavelength 1.541551 Å.

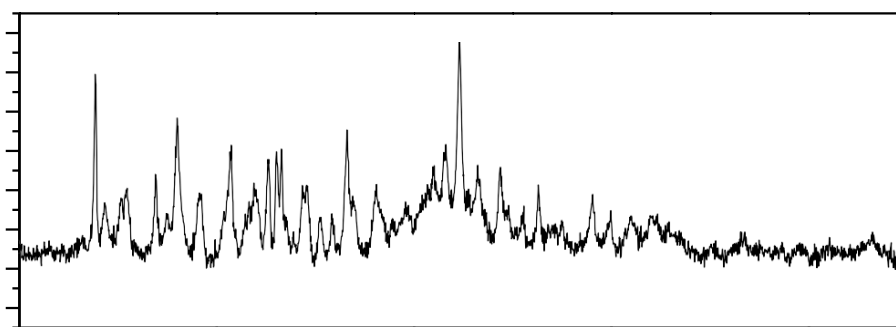


**Figure 3.** Powder X-ray diffractogram pattern of [Ru(L)<sub>2</sub>].

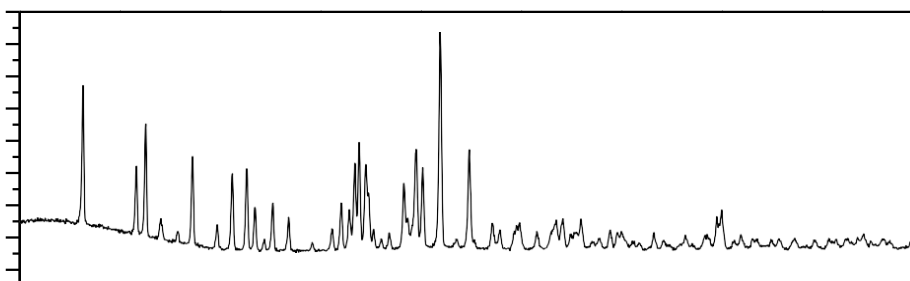


**Figure 4.** Powder X-ray diffractogram pattern of [Cd(L)<sub>2</sub>(H<sub>2</sub>O)<sub>2</sub>].

**Table 5.** X-ray diffractogram data of Ru(II) and Cd (II) complexes.

Parameters	[Ru(L) <sub>2</sub> ]	[Cd(L) <sub>2</sub> (H <sub>2</sub> O) <sub>2</sub> ]
Temperature	298K	298K
Wavelength (Å)	1.541551	1.541551
Radiation	CuKα	CuKα
Crystal system	Triclinic	Monoclinic
Unit Cell Dimension		
a(Å)	9.68646	14.4806
b(Å)	14.8043	16.9521
c(Å)	17.0610	19.4501
α(°)	101.75	90
β(°)	100.29	106.21
γ(°)	100.873	90
Average particle size (nm)	21.051401	14.923426

The unit cell parameters and calculations were performed using powder-X software. The average particle size was calculated using grain software [26]. Table 5 gives the summary of unit cell parameters and average particle size. Miller's indices and the calculated lattice constants correspond to the triclinic system for Ru(II) and the monoclinic for Cd(II) complexes are shown in Figures 3 and 4.

### 3.6. Antimicrobial activity.

The in vitro antimicrobial screening of synthesized ligand and metal complexes was tested against four bacteria (*S. aureus*, *S. pyogenes*, *E. coli*, and *S. typhi*) and two fungi (*C. albicans* and *T. rubrum*) by petri-plate containing 30 ml potato dextrose agar and nutrient agar medium, the plates were incubated for 20-24 hr and 24-48 hr for bacteria and fungi stains, respectively. The activities were measured in terms of the zone of inhibition in mm. Cefotaxime, Azithromycin, and Clotrimazole were used as standard drugs for bacteria and fungi, respectively, at 500 ppm concentration of sample as well as drugs.

The metal complexes exhibit higher inhibition against tested microorganisms than the free ligand. The value in the above table indicates that the activity of the Schiff base ligand became more pronounced when coordinated with the metal ions. The presence of azomethine moiety and chelation effect with central metal enhances the antibacterial activities [27]. This enhancement in the antibacterial activity of these metal complexes can be explained based on the chelation theory.

**Table 6.** Results of antimicrobial activity of synthesized compounds.

Compounds	Zone of Inhibition in mm					
	Gm +ve bacteria		Gm -ve bacteria		Antifungal activity	
	<i>S. aureus</i>	<i>S. pyogenes</i>	<i>E. coli</i>	<i>S. typhi</i>	<i>C. albicans</i>	<i>T. rubrum</i>
Ligand (L)	08	08	09	10	08	9
[Ru(L) <sub>2</sub> ]	09	08	09	08	09	10
[Rh(L) <sub>2</sub> ]	11	10	12	12	10	09
[Ag(L) <sub>2</sub> (H <sub>2</sub> O) <sub>2</sub> ]	16	14	15	16	19	21
[Cd(L) <sub>2</sub> (H <sub>2</sub> O) <sub>2</sub> ]	18	16	16	14	18	20
<b>Cefotaxime</b>	-	-	<b>26</b>	<b>20</b>	-	-
<b>Azithromycin</b>	<b>24</b>	<b>26</b>		-	-	-
<b>Clotrimazole</b>	-	-	-	-	<b>14</b>	<b>16</b>

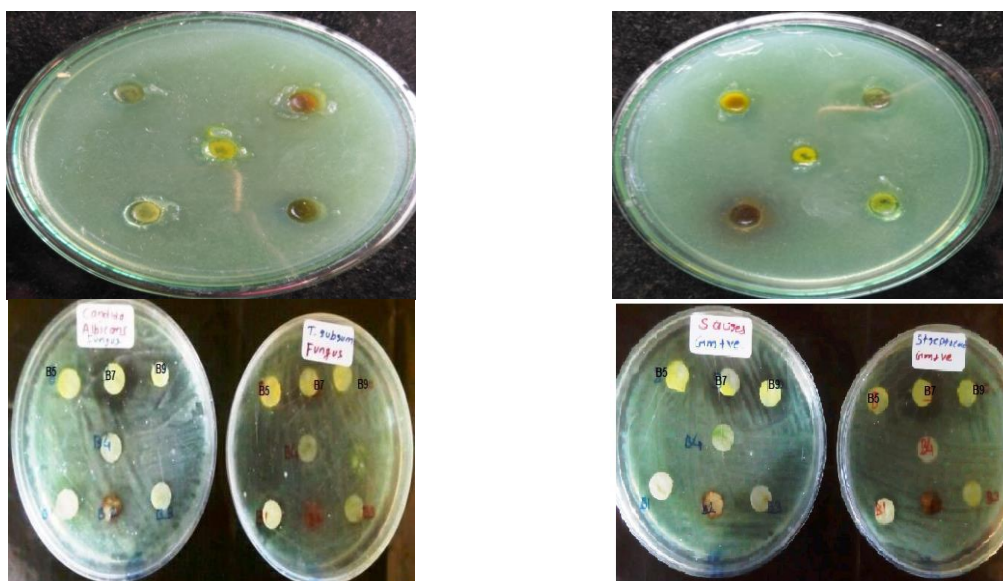


**Figure 5.** Selected images of antimicrobial activity of ligands L its metal complexes.

When a metal ion is chelated with a ligand, its polarity will be reduced to a greater extent due to the overlap of ligand orbital and the partial sharing of the positive charge of the metal ion with donor groups. Furthermore, the chelation process increases the delocalization of the  $\pi$ -electrons over the whole chelate ring, which results in an increase in the lipophilicity of the metal complexes. Consequently, the metal complexes can easily penetrate the lipid membranes and block the metal binding sites of enzymes of the microorganisms. These metal complexes also affect the respiration process of the cell and thus block the synthesis of proteins, which restrict further growth of the organism. The antimicrobial activity of ligand and metal complexes is shown in Table 6.

#### 4. Conclusion

In the present work, Ru (III), Rh(II), Pd(II), Ag(II), And Cd(II) complexes were prepared from 6-iodo-4-oxo-4H-chromene-3-carbaldehyde and 4-Methyl-1,2,3-thiadiazole-5-carbohydrazide. These Schiff base are characterized using various spectral techniques. IR spectra revealed the coordination of Schiff base ligand with metal ions through azomethine nitrogen, chromone moiety's carbonyl oxygen, and hydrazide moiety's carbonyl oxygen. The structural elucidation studies by various spectral techniques (IR, TGA, and  $^1\text{H}$  NMR) suggested that the nature of the ligand is tridentate and that the metal complexes' geometry is octahedral. Thermogravimetric analysis studies demonstrate the stability of complexes and provide the number of coordinated water molecules. Antimicrobial studies suggest that Schiff base and its complexes play a vital role in developing a new class of antibiotics.

#### Funding

This research received no external funding.

#### Acknowledgments

The authors are thankful to the Head of the Department of Chemistry and the Principal for providing the laboratory facilities. MSS'S Arts Science and Commerce College, Ambad, India, for their support.

#### Conflicts of Interest

The authors declare no conflict of interest.

#### References

1. Ibrahim, F.M.; Abdalhadi, S.M. Performance of Schiff bases metal complexes and their ligand in biological activity: a review. *Al-Nahrain J. Sci.* **2021**, *24*, 1-10, <https://doi.org/10.22401/ANJS.24.1.01>.
2. Abubakar, T.; Haruna, A.; Isyaku, S.; Imam, M. Microwave-Assisted Synthesis, Characterization And Antimicrobial Activity Of Copper (Ii) Complex With Salicylaldehyde And P-Chloroaniline Schiff Base. *Bayero J. Pure Appl. Sci.* **2022**, *13*, 117-122, <https://doi.org/10.4314/bajopas.v13i1.21S>.
3. Undegaonkar, M.G.; Moharir, S.P.; Bhosale, V.N.; Mirgane, S.R. Microwave Assisted Synthesis, Characterization and Bioactivity Study of Binuclear Complexes of Schiff base derived from 2-Amino-5, 6-dimethyl benzimidazole and Terephthalaldehyde. *J. Chem. Chem. Sci.* **2021**, *11*, 33-42.
4. Kumar, S.S.; Biju, S.; Sadasivan, V. Synthesis, structure characterization and biological studies on a new aromatic hydrazone, 5-(2-(1,5-dimethyl-3-oxo-2-phenyl-2,3-dihydro-1H-pyrazol-4-yl)hydrazono)-2,2-dimethyl-1,3-dioxane-4,6-dione, and its transition metal complexes. *J. Mol. Struct.* **2018**, *1156*, 201-209, <https://doi.org/10.1016/j.molstruc.2017.11.057>.

5. Khattab, T.A.; Allam, A.A.; Othman, S.I.; Bin-Jumah, M.; Al-Harbi, H.M.; Fouda, M.M.G. Synthesis, Solvatochromic Performance, pH Sensing, Dyeing Ability, and Antimicrobial Activity of Novel Hydrazone Dyestuffs. *J. Chem.* **2019**, *2019*, 7814179, <https://doi.org/10.1155/2019/7814179>.
6. Ramaiah, K.; Prashanth, J.; Haribabu, J.; Srikanth, K.E.; Venkatram Reddy, B.; Karvembu, R.; Laxma Reddy, K. Vibrational spectroscopic (FT-IR, FT-Raman), anti-inflammatory, docking and molecular characteristic studies of Ni(II) complex of 2-aminonicotinaldehyde using theoretical and experimental methods. *J. Mol. Struct.* **2019**, *1175*, 769-781, <https://doi.org/10.1016/j.molstruc.2018.08.044>.
7. Vinusha, H.; Kollur, S.P.; Ramu, R.; Shirahatti, P.S.; Prasad, N.; Begum, M. Chemical Synthesis, Spectral Characterization and Biological Investigations of Novel Triazole-Based Schiff Base Ligand and its Transition Complexes. *Lett. Appl. NanoBioScience* **2020**, *9*, 1372-1388, <https://doi.org/10.33263/LIANBS93.13721388>.
8. Ali, I.; Mahmood, L.M.A.; Mehdar, Y.T.H.; Aboul-Enein, H.Y.; Said, M.A. Synthesis, characterization, simulation, DNA binding and anticancer activities of Co(II), Cu(II), Ni(II) and Zn(II) complexes of a Schiff base containing o-hydroxyl group nitrogen ligand. *Inorg. Chem. Commun.* **2020**, *118*, 108004, <https://doi.org/10.1016/j.inoche.2020.108004>.
9. Ambika, S.; Manojkumar, Y.; Arunachalam, S.; Gowdhami, B.; Meenakshi Sundaram, K.K.; Solomon, R.V.; Venuvanalingam, P.; Akbarsha, M.A.; Sundararaman, M. Biomolecular Interaction, Anti-Cancer and Anti-Angiogenic Properties of Cobalt(III) Schiff Base Complexes. *Sci. Rep.* **2019**, *9*, 2721, <https://doi.org/10.1038/s41598-019-39179-1>.
10. Liu, F.; Jin, P.; Gong, H.; Sun, Z.; Du, L.; Wang, D. Antibacterial and antibiofilm activities of thyme oil against foodborne multiple antibiotics-resistant *Enterococcus faecalis*. *Poul. Sci.* **2020**, *99*, 5127-5136, <https://doi.org/10.1016/j.psj.2020.06.067>.
11. Song, Y.J.; Yu, H.H.; Kim, Y.J.; Lee, N.-K.; Paik, H.-D. Anti-biofilm activity of grapefruit seed extract against *Staphylococcus aureus* and *Escherichia coli*. *J. Microbiol. Biotechnol.* **2019**, *29*, 1177-1183, <https://doi.org/10.4014/jmb.1905.05022>.
12. Hamzah, H.; Yudhawan, I.; Rasdianah, N.; Setyowati, E.; Nandini, E.; Utami, S.; Pratiwi, T. Clove oil has the activity to inhibit middle, maturation and degradation phase of *Candida tropicalis* biofilm formation. *Biointerface Res. Appl. Chem.* **2022**, *12*, 1507-1519, <https://doi.org/10.33263/BRIAC122.15071519>.
13. Sharma, G.; Gupta, H.; Dang, S.; Gupta, S.; Gabrani, R. Characterization Of Antimicrobial Substance With Antibiofilm Activity From *Pediococcus acidilactici*. *J. Microbiol. Biotechnol. Food Sci.* **2021**, *9*, 979-982, <https://doi.org/10.15414/jmbfs.2020.9.5.979-982>.
14. Bhale, S.P.; Yadav, A.R.; Tekale, S.U.; Nawale, R.B.; Marathe, R.P., Kendrekar, P.S.; Pawar, R.P. Synthesis, Characterization and Antimicrobial Screening of Novel Hydrazone Ligand & Its Transition Metal Complexes. *Asian Journal of Chemistry* **2019**, *31*, 938-942, <https://doi.org/10.14233/ajchem.2019.21795>.
15. Venugopal, N.; Krishnamurthy, G.; Bhojyanaik, H.S.; Madhukar Naik, M.; Sunilkumar, N. Synthesis, characterization, and biological activity of Cu(II) and Co(II) complexes of novel N1,N2-bis(4-methyl quinolin-2-yl)benzene-1,2-diamine: CuO and CoO nanoparticles derived from their metal complexes for photocatalytic activity. *Inorg. Nano-Met. Chem.* **2021**, *51*, 1117-1126, <https://doi.org/10.1080/24701556.2020.1814337>.
16. Dong, X.; Xie, S.; Zhu, J.; Liu, H.; Zhao, Y.; Ni, T.; Wu, L.; Zhu, Y. Mesoporous CoO<sub>x</sub>/C Nanocomposites Functionalized Electrochemical Sensor for Rapid and Continuous Detection of Nitrite. *Coatings* **2021**, *11*, 596, <https://doi.org/10.3390/coatings11050596>.
17. Ndala, A.; Itota, B.; Chamier, J.; Ray, S.; Sunday, C.; Chowdhury, M. Novel (CH<sub>6</sub>N<sub>3</sub><sup>+</sup>, NH<sub>3</sub><sup>+</sup>)-functionalized and nitrogen doped Co<sub>3</sub>O<sub>4</sub> thin film electrochemical sensor for nanomolar detection of nitrite in neutral pH. *Electrochim. Acta* **2021**, *388*, 138556, <https://doi.org/10.1016/j.electacta.2021.138556>.
18. Ranjitha, N.; Krishnamurthy, G.; Manjunatha, M.N.; Naik, H.S.B.; Pari, M.; K, V.N.; Lakshmikantha, J.; Pradeepa, K. Electrochemical determination of glucose and H<sub>2</sub>O<sub>2</sub> using Co(II), Ni(II), Cu(II) complexes of novel 2-(1,3-benzothiazol-2-ylamino)-N-(5-chloro-2-hydroxyphenyl)acetamide: Synthesis, structural characterisation, antimicrobial, anticancer activity and docking studies. *J. Mol. Struct.* **2023**, *1274*, 134483, <https://doi.org/10.1016/j.molstruc.2022.134483>.
19. Pawar, D.C.; Gaikwad, S.V.; Kamble, S.S.; Gavhane, P.D.; Gaikwad, M.V.; Dawane, B.S. Design, synthesis, docking and biological study of pyrazole-3, 5-diamine derivatives with potent antitubercular activity. *Chem. Methodol* **2022**, *6*, 677-690, <https://doi.org/10.22034/CHEMM.2022.343572.1538>.
20. Wong, K.T.; Osman, H.; Parumasivam, T.; Supratman, U.; Che Omar, M.T.; Azmi, M.N. Synthesis, Characterization and Biological Evaluation of New 3,5-Disubstituted-Pyrazoline Derivatives as Potential

- Anti-*Mycobacterium tuberculosis* H37Ra Compounds. *Molecules* **2021**, *26*, 2081, <https://doi.org/10.3390/molecules26072081>.
21. Saikumari, N. Synthesis and characterization of amino acid Schiff base and its copper (II) and its antimicrobial studies. *Mater. Today: Proc.* **2021**, *47*, 1777-1781, <https://doi.org/10.1016/j.matpr.2021.02.607>.
  22. El-Gammal, O.A.; Saad, D.A.; Al-Hossainy, A.F. Synthesis, spectral characterization, optical properties and X-ray structural studies of S centrosymmetric N<sub>2</sub>S<sub>2</sub> or N<sub>2</sub>S<sub>2</sub>O<sub>2</sub> donor Schiff base ligand and its binuclear transition metal complexes. *J. Mol. Struct.* **2021**, *1244*, 130974, <https://doi.org/10.1016/j.molstruc.2021.130974>.
  23. Das, A.; Rajeev, A.; Bhunia, S.; Arunkumar, M.; Chari, N.; Sankaralingam, M. Synthesis, characterization and antimicrobial activity of nickel(II) complexes of tridentate N<sub>3</sub> ligands. *Inorganica Chim. Acta* **2021**, *526*, 120515, <https://doi.org/10.1016/j.ica.2021.120515>.
  24. Sunil, S.V.; Kerima, O.Z.; Santosh-Kumar, H.S.; Prabhakar, B.T.; Pramod, S.N.; Niranjana, P. In Silico Characterization of a Transcript Code Based Screening of Antimicrobial Peptide from *Trichogramma chilonis*. *International Journal of peptide and Therapeutics* **2021**, *27*, 2861-2872, <https://doi.org/10.1007/s10989-021-10295-9>.
  25. Sunil, S.V.; Kerima, O.Z.; Kumar, H.S.S.; Prabhakar, B.T.; Pramod, S.N.; Niranjana, P. In Silico Characterization of a Transcript Code Based Screening of Antimicrobial Peptide from *Trichogramma chilonis*. *Int. J. Pept. Res. Ther.* **2021**, *27*, 2861-2872, <https://doi.org/10.1016/j.molstruc.2020.129669>.
  26. Joshi, N.; Gore, V.; Tekale, S.; Nawale, R.; Rajani, D.; Bembalkar, S.; Pawar, R. Synthesis and Biological Evaluation Study of New Bis-imine Ligand and Metal Complexes. *Lett. Appl. NanoBioSci.* **2021**, *10*, 2207-2214, <https://doi.org/10.33263/LIANBS102.22072214>.
  27. Sahoo, J.; Parween, G.; Sahoo, S.; Mekap, S.K.; Sahoo, S.; Paidasetty, S.K. Synthesis, spectral characterization, in silico and in vitro antimicrobial investigations of some Schiff base metal complexes derived from azo salicylaldehyde analogues. *Indian J. Chem.* **2016**, *55*, 1267-1276.